Journal of Power Sources 196 (2011) 3868–3873

Contents lists available at ScienceDirect

Journal of Power Sources

journal homepage: www.elsevier.com/locate/jpowsour

Electrodeposited porous-microspheres Li–Si films as negative electrodes in lithium-ion batteries

Rongguan Lv, Jun Yang*, Jiulin Wang, Yanna NuLi

School of Chemistry and Chemical Engineering, Shanghai Jiao Tong University, Shanghai 200240, China

ARTICLE INFO

Article history:
Received 14 October 2010
Received in revised form
13 December 2010
Accepted 28 December 2010
Available online 12 January 2011

Keywords:
Porous Li–Si film
Electrodeposition
Negative electrode
Lithium-ion battery

ABSTRACT

A porous-microspheres Li–Si film (PMLSF) is prepared by multi-step constant current (MSCC) electrodeposition on Cu foil. Its structure and morphology are characterized using X-ray diffraction (XRD) and scanning electron microscope (SEM). As negative electrodes of lithium-ion batteries, the PMLSF electrode delivers the first gravimetric and geometric charge capacities of 2805.7 mA h g^{-1} and 621.9 μA h cm^{-2} at the current density of 25.5 μA cm^{-2}, and its initial coulombic efficiency is as high as 98.2%. When the PMLSF electrode is cycled in VC-containing electrolyte, the superior cycling performance can be obtained. After 50 cycles, 96.0% of its initial capacity is retained at the current density of 50.0 μA cm^{-2}. Electrochemical impedance spectra (EIS) research confirms the positive effect of VC additive on the behavior of the PMLSF electrode.

1. Introduction

Compact power sources are critical components of modern electronics. The thin-film lithium-ion battery is one of the most favorite options because it can provide a high energy and power density [1]. Recenly, they have been used in smartcards, implantable medical devices, microelectromechanical systems (MEMS), and others [2]. However, the theoretical Li-storage capacity of commercial carbon anodes is limited to 372 mA h g^{-1}; thus there is a great interest in developing alternative anode materials to carbonaceous. Silicon is a promising candidate for next-generation anodes due to its low discharge potential vs. Li/Li^+ and high theoretical Li-storage capacity of 4200 mA h g^{-1} [3]. Nevertheless, Si electrodes suffer from poor electrochemical reversibility upon cycling caused by a drastic volume change of Si (>300%) during the lithium insertion/extraction process.

To reduce the absolute volume change and improve the cycling stability of Si electrode, various Si nanostructures have been proposed and compatible electrolytes (e.g. vinylene carbonate (VC) as additive) have been studied [4–7]. Si and Si-based alloy thin films become one of the important objects of study. These thin films are generally prepared by physical or chemical evaporation/deposition techniques. Takamura et al. reported a vacuum-deposited phosphor-doped n–Si film with thickness of 50 nm on a Ni foil, which showed a reversible capacity as high as 3000 mA h g^{-1} for 1000 cycles in a lithium-ion battery [8]. Fleischauer and co-workers prepared porosity-controlled Si thin films by the glancing angle deposition (GLAD) technique. This film was composed of numerous Si columns with a uniform interspace. The peculiar morphology of the Si thin film led to good electrochemical performance. A 500-nm thick Si thin film with a porosity of ca. 80% presented a reversible capacity of over 90 μA h cm^{-2} and good capacity retention (75 μA h cm^{-2} after 70 cycles) [1]. The Seong group proposed Si–Sn nanocomposite electrodes fabricated by an RF-magnetron sputtering technique. The capacity could retain 560 μA h cm^{-2} μm^{-1} after 15 cycles, and the available capacity was dependent on the amount of the incorporated Sn [9]. It is also noticed that most of the Si or Si-based thin film electrodes have unsatisfactory coulombic efficiency at the first cycle, which mainly originatd from the formation of a solid electrolyte interphase (SEI) on the electrode surface [1,8–12].

The initial coulombic efficiency can be actually improved by preforming an artificial SEI layer (through chemical modification) on the active materials and/or prelithiating the active materials [13–16]. For example, Seong et al. studied lithiation of silicon monoxide using Li powders. Although the batteries showed enhanced initial reversibility and coulombic efficiency, the bulk distribution of Li powders in electrode was not uniform [15]. In this article, porous-microspheres Li–Si films (abbreviated as PMLSF hereafter) were first electrodeposited on Cu foil from propylene carbonate (PC) solution containing tetrachlorosilane ($SiCl_4$) and lithium perchlorate ($LiClO_4$) and exhibited high initial coulombic

* Corresponding author at: School of Chemistry and Chemical Engineering, Shanghai Jiao Tong University, 800 Dongchuan Road, Shanghai 200240, China.
Tel.: +86 21 5474 7667; fax: +86 21 5474 7667.
E-mail address: Yangj723@sjtu.edu.cn (J. Yang).

0378-7753/$ – see front matter © 2011 Elsevier B.V. All rights reserved.
doi:10.1016/j.jpowsour.2010.12.101

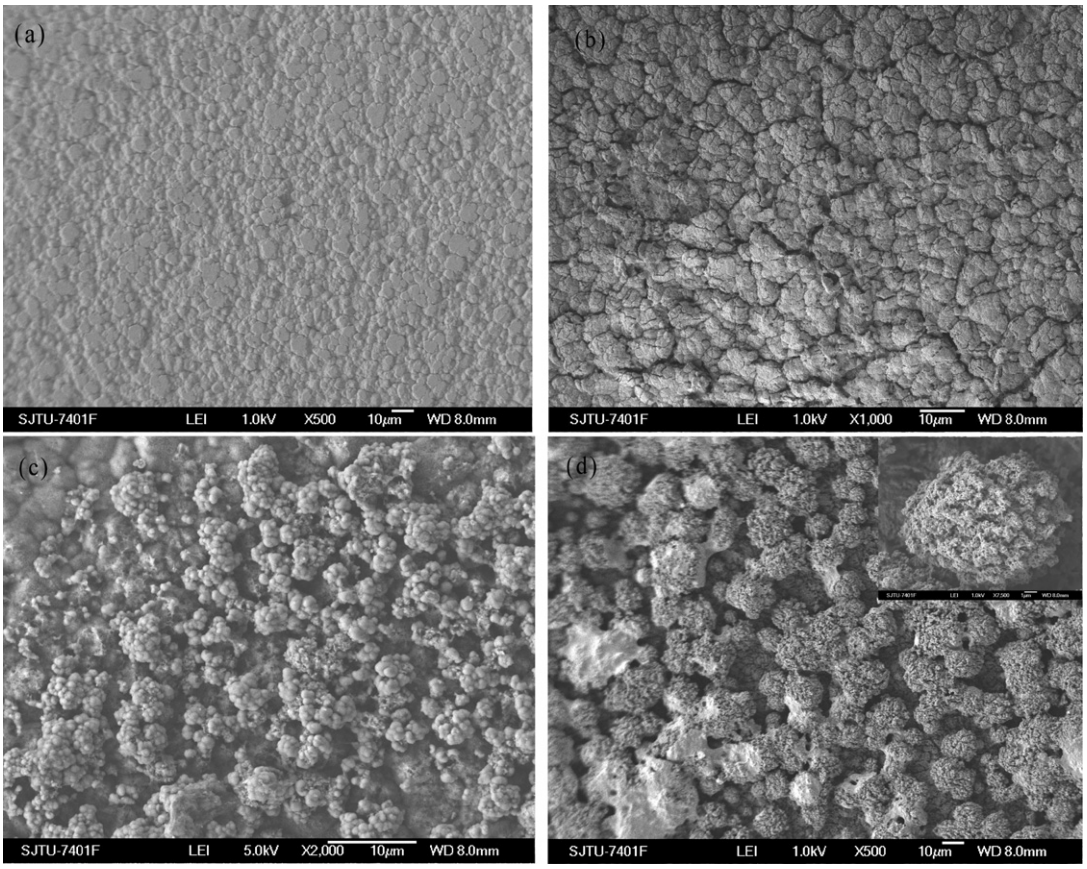

Fig. 1. SEM images of Cu foil substrate (a), electrodeposited Si thin film (b), primary Li–Si deposit (c), and PMLSF electrode (d) (the inset shows its partial magnification).

efficiency and cycling stability as negative electrodes for lithium-ion battery.

2. Experimental

All experiments were carried out in an Ar-filled glove box at $30 \pm 1\,^{\circ}C$. $SiCl_4$ and $LiClO_4$ were added to the organic electrolyte as Si source and Li source, respectively. PC was chosen as an organic solvent because of its high $SiCl_4$ and $LiClO_4$ solubility. These chemicals were used without a further purification. The electrolyte composition was adjusted to $0.5\,mol\,L^{-1}$ $SiCl_4$ and $0.6\,mol\,L^{-1}$ $LiClO_4$ in PC. For a comparison, Si thin film was electrodeposited in PC solution containing $0.5\,mol\,L^{-1}$ $SiCl_4$ and $0.1\,mol\,L^{-1}$ tetrabutylammonium chloride as supporting electrolyte.

A conventional three-electrode cell was employed for the electrodeposition experiments. 25-μm Cu foil with a geometric surface area of $0.785\,cm^2$ ($\phi = 1.0\,cm$) was used as the substrate (cathode) for PMLSF electrodeposition. A polished graphite plate was employed as the counter electrode (anode). Cu foil and graphite plate were ultrasonically cleaned in acetone, subsequently washed with oxalic acid ($0.1\,mol\,L^{-1}$) and distilled water, and dried under vacuum at 50 °C. Platinum wire served as a quasi-reference electrode. PMLSF and Si thin films were electrodeposited on one side of the Cu foil on an electrochemical workstation CHI660C (Chenhua Co., China). Multi-step constant current (MSCC) electrolysis for PMLSF and Si thin films was conducted at the current density of $-3.82\,mA\,cm^{-2}$ for 10 min, followed by the current density of $-1.27\,mA\,cm^{-2}$ for 150 min. All freshly deposited samples were rinsed with PC, and then directly characterized and electrochemically evaluated.

The PMLSF before cycling and after 50 discharge–charge cycles were analyzed by X-ray diffraction (XRD) on a Rigaku diffractometer D/MAX-2200/PC equipped with Cu K_α radiation. Parafilm covered the surface of a PMLSF to keep out the air during XRD experiments. The morphologies of the samples were observed by scanning electron microscopy (SEM) on a JEOL field-emission microscope (JSM-7401F). The composition was determined by inductively coupled plasma (ICP) measurements (Hitachi P-4010, Japan). The gravimetric capacity of PMLSF electrode was calculated according to the weight of silicon in the PMLSF obtained from the ICP analysis.

Electrochemical behaviors were evaluated using CR2016 coin cells assembled in an Ar-filled glove box (Mbraun, Germany). The test cell was composed of PMLSF or Si film working electrode and Li foil counter electrode. The electrolyte consisted of a solution of $1\,mol\,L^{-1}$ $LiPF_6$ in EC/DMC (1:1 vol%) with or without 2 wt% VC as additive. ENTEK ET20-26 served as membrane separator. The cells were charged (delithiation) and discharged (lithiation) using LAND CT2001A system in a galvanostatic mode between 0.01 and 1.4 V vs. Li/Li^+. For the first pre-cycle, the current density of $25.5\,\mu A\,cm^{-2}$ was adopted following by the current density of $50.0\,\mu A\,cm^{-2}$. Cyclic voltammogram (CV) of a PMLSF electrode was measured at the range of 0.01–1.5 V vs. Li/Li^+ at a scan rate of $0.2\,mV\,s^{-1}$. Electrochemical impedance spectra (EIS) were taken on CHI660C over the frequency range from 100 kHz to 0.01 Hz with ac amplitude of 5 mV.

3. Results and discussion

Due to the high activity, the deposited PMLSF electrodes were preserved under Ar before transporting to the SEM, XRD and ICP apparatus. ICP composition analysis for the deposit indicates the presence of Li and Si elements in PMLSF. The Si/Li atomic ratio of the deposit layer is about 1.51 (85.9 wt% for Si) at the first electrodepo-

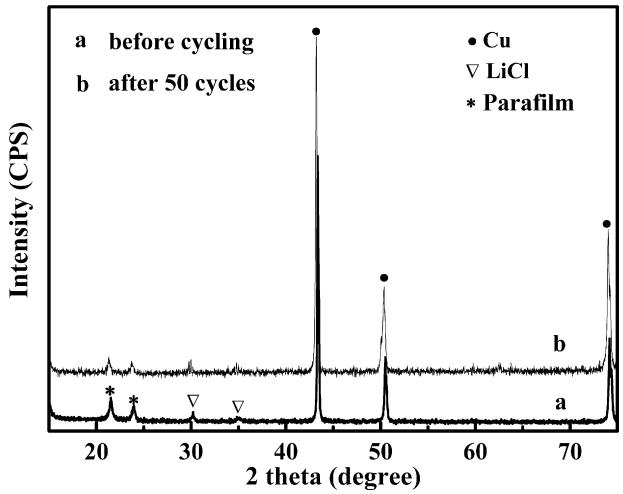

Fig. 2. XRD patterns of PMLSF deposited on Cu foil before and after 50 cycles in VC-containing electrolyte.

sition stage using the current density of −3.82 mA cm^{-2} for 10 min. After the second stage using the current density of −1.27 mA cm^{-2} for 150 min, the Si/Li atomic ratio decreases to about 0.46 (65.0 wt% for Si) in PMLSF. It means that more silicon is deposited during the initial electrochemical process. With continuous deposition, lithium content rises. In view that Si can electrochemically alloy with lithium, the early deposited Si will induce the reduction of lithium, leading to the higher lithium content. The co-deposition of lithium is favorable for an increase of the electronic conductivity and growth of the deposit layer. The cross-section SEM measurement indicates that the thickness of the PMLSF is about 15 μm, thicker than that of electrodeposited Si thin film (several micrometers).

Fig. 1 shows the SEM images of Cu foil substrate, electrodeposited Si thin film, and Li–Si deposits at different electrodeposition stages. Cu foil demonstrates a rough and concavo-convex morphology (Fig. 1a), which is beneficial to good adhesion of the Li–Si deposited layer on it. At the early stage of electrodeposition, many fine Li–Si spherules (<1 μm) with higher Si content aggregated and covered Cu substrate (Fig. 1c). In the subsequent process, more lithium was deposited and part of it may alloy with Si, causing the primary particles to expand. The aggregates (the second particles) grew to become inter-connected porous particles from several micrometers to several tens of micrometers (Fig. 1d). Finally, the PMLSF was formed. The porous structure may be related to the gas bubbles arising from the reductive decomposition of PC solvent on the fresh Li-rich surface of the electrode [17]. Small amount of mini-bubbles can be observed carefully on the cathode during the experiment. They might act as a soft template during electrodeposition process and create a continuous path from the aggregated particles to the electrolyte interface [18]. The electrodeposition stops in the places where the bubbles occupy. Thus, numerous pores are formed in the particles. By contrast, the Si thin film demonstrates compact particle morphology without any pores (Fig. 1b). This could be explained by that the newly deposited Si cannot cause the reduction of PC.

Fig. 2 presents the XRD patterns of the deposited PMLSF electrode before cycling and after 50 discharge–charge cycles. No peaks can be detected for Si, Li or Li–Si alloy except weak peaks of LiCl, which indicates that the electrodeposited PMLSF is in an amorphous or nano-crystalline state and its structure can be maintained during cycling. LiCl impurity may come from the reaction of freshly electrodeposited lithium and/or Li–Si alloy with a small amount of chlorine in the electrolyte diffusing from the anode. As shown in Fig. 2b, LiCl impurity remains after 50 cycles, indicating its inertia in the electrode.

The lithium insertion/extraction reaction of the PMLSF electrode was investigated by the cyclic voltammetry (CV). The open-circuit potential of the electrode was about 0.4 V vs. Li/Li$^+$ before cycling, compared with 2.6 V vs. Li/Li$^+$ for deposited Si film electrode. This indicates that part of lithium in the PMLSF electrode is reactive. In the first cathodic scan, a sharp peak located at 0.01 V vs. Li/Li$^+$ as shown in Fig. 3 can be assigned to the formation of Li-rich phases. The anodic scan exhibits two peaks at about 0.39 and 0.53 V vs. Li/Li$^+$, which is related to the de-alloying process. After the first cycle, the anodic peak located at 0.53 V vs. Li/Li$^+$ shifts to the lower potential of 0.49 V vs. Li/Li$^+$, while the cathodic peak shifts to more positive potential. The electrochemical polarization declines via the first lithium insertion/extraction cycle. However, none of the apparent peaks related with SEI formation can be observed in the cathodic scans above 0.4 vs. Li/Li$^+$ in VC-free or VC-containing (not shown here) electrolyte, which means that a SEI layer may have been formed before electrochemical cycling test.

Fig. 4 shows the discharge–charge curves of the PMLSF and Si film electrodes in VC-free electrolyte at the current density of 25.5 (only for the 1st cycle) and 50.0 μA cm^{-2}, respectively. For the PMLSF electrode, the sloped discharge and charge trends confirm its amorphous structure. The lithiation and delithiation take place in a voltage range of 0.2–0.01 V and 0.1–0.6 V vs. Li/Li$^+$, respectively, which is consistent with the result from CV (Fig. 3). The first discharge capacity is 2858.5 mA h g^{-1} or 633.6 μA h cm^{-2}, and the first charge capacity is 2805.7 mA h g^{-1} or 621.9 μA h cm^{-2}, educing a coulombic efficiency of 98.2%. On the contrary, the Si film electrode presents very low coulombic efficiency of 26.7% at the 1st cycle and small cycle capacity. Its poor performance may be attributed to the dense morphology, limited thickness due to the poor electronic conductivity and high impurity content [19,20]. From this point of view, co-deposition of lithium and silicon is very effective for creating a good anode for lithium ion battery.

Judging from the coulombic efficiency, the previous co-deposited lithium cannot be extracted in cell cycling. However, this part of lithium compensates the irreversible capacity caused by the formation of SEI film related to electrolyte decomposition, the structure defects of Si host and irreversible reduction of reactive impurities in the deposit layer. The ICP measurement showed that the Si/Li atomic ratio in PMLSF changed from 0.46 to 0.42 after 50 discharge–charge cycles in VC-containing electrolyte. It should be realized that any change of lithium content at this stage is related not only to the PMLSF, but also to the SEI film.

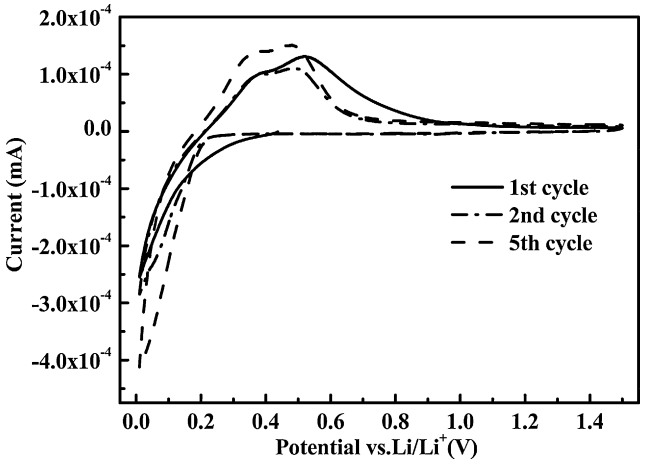

Fig. 3. Cyclic voltammogram of the PMLSF electrode in VC-free electrolyte at a scan rate of 0.2 mV s^{-1}.

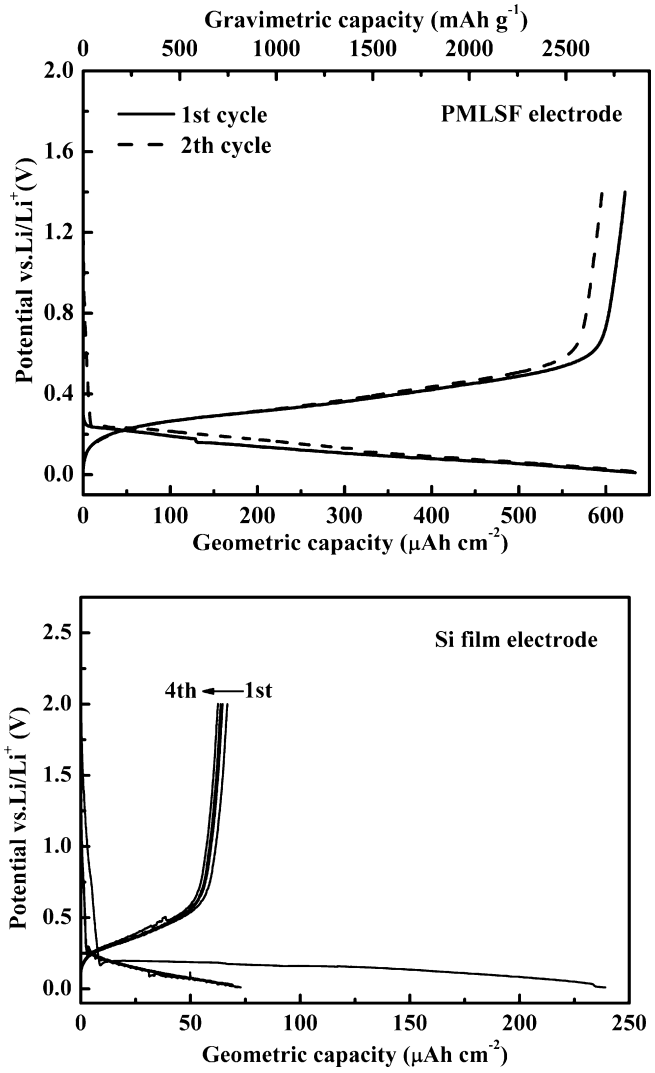

Fig. 4. The discharge/charge plots of PMLSF and Si film electrodes in VC-free electrolyte at the current density of 25.5 (only for the 1st cycle) and 50 μA cm^{-2}, respectively.

Fig. 5a shows the discharge–charge cycling performance of the PMLSF electrode in VC-free and VC-containing electrolytes. It can be observed that the initial discharge and charge capacity in VC-free electrolyte are 646.8 μA h cm^{-2} and 595.5 μA h cm^{-2}, respectively. After 50 cycles, its charge capacity is 479.7 μA h cm^{-2}, retaining 80.6% of its initial capacity. Maranchi et al. reported that reversible capacity of 1-μm-thick dense Si film faded substantially after 12 cycles [21]. Superior cycling stability of the PMLSF electrode can be partly attributed to its unique porous particle structure and inter-particle free space, which can accommodate a part of the volume change during lithium insertion/extraction and favor the structural stability. However, the volume effect could not be entirely avoided, which resulted in capacity loss of 0.39% per cycle. By contrast, an excellent cycling performance can be achieved in a VC-containing electrolyte. The reversible charge capacity retains more than 96.0% of its first capacity after 50 cycles. Fig. 5b further shows the influence of the charge–discharge current density on the capacity retention. With the enhanced current density, the capacity decreases regularly. The reversible capacity decreases from ~600 μA h cm^{-2} at the current density of 50.0 μA cm^{-2} to ~550 μA h cm^{-2} at the current density of 125 μA cm^{-2}. Moreover, the capacity can be recovered when the current density returns to 50.0 μA cm^{-2}, indicating that the PMLSF electrode has a good electrochemical reversibility and structural integrity.

To elucidate the reason for the improved stability of a PMLSF electrode in VC-containing electrolyte, electrochemical impedance spectra (EIS) were studied. The Nyquist plots of the PMLSF electrode charged to 1.4 V vs. Li/Li$^+$ in VC-free and VC-containing electrolytes after 1 and 10 cycles are shown in Fig. 6. A depressed semicircle at high frequencies (HFr) and a straight line at low frequencies (LFr) can be observed for all the Nyquist plots, which are similar to previously reported results of Si thin film electrode [7]. The diameter of the depressed semicircle mainly represents interfacial resistance for electrochemical reaction and the straight line is related to a diffusion controlled process [22]. Compared with Fig. 6a and b, it can be noticed that the diameter of HFr semicircle after 1 cycle in VC-containing electrolyte is larger than that in VC-free electrolyte. This indicates the higher resistance of the SEI layer in VC-containing electrolyte, which derives from a thicker and/or denser layer structure formed on the surface of the PMLSF electrode. It is more notable that the change of HFr semicircle during cycling is totally different in both the electrolytes. The enlarged HFr semicircle in VC-free electrolyte with increased cycle number implies the enhanced interfacial resistance for the electrochemical reaction, leading to the deterioration of the PMLSF electrode. On the contrary, the diameter of HFr semicircle becomes smaller upon cycling in VC-containing electrolyte and the slope of LFr straight line is almost unaltered after 10 cycles, which may be explained

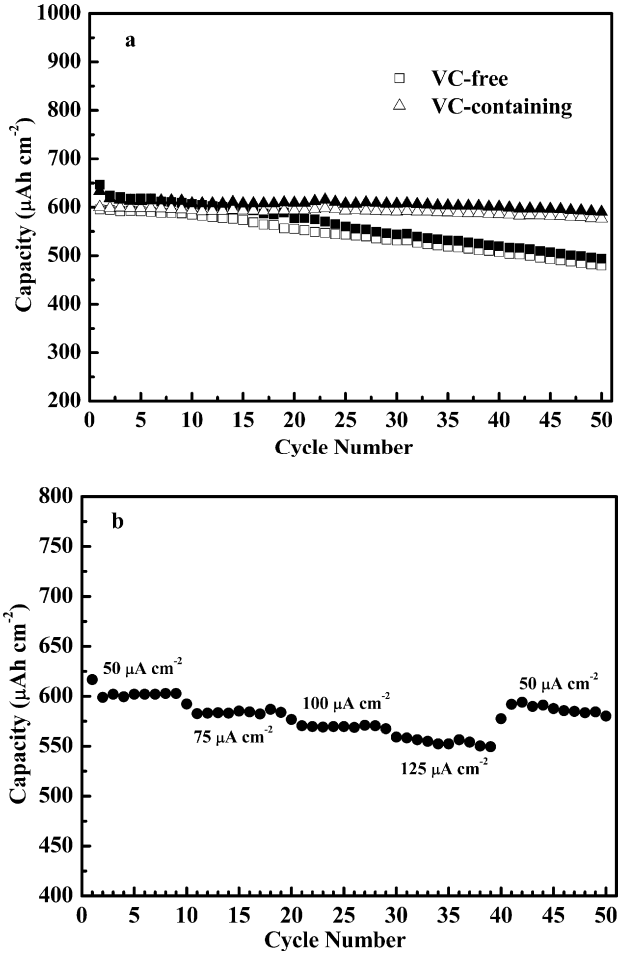

Fig. 5. Cycling behaviors of the PMLSF electrodes in VC-free and VC-containing electrolytes at the current density of 50.0 μA cm^{-2} (a) and the reversible capacities during continuous cycling at various current density in VC-containing electrolyte (b). Solid and hollow marks represent discharge and charge capacities, respectively.

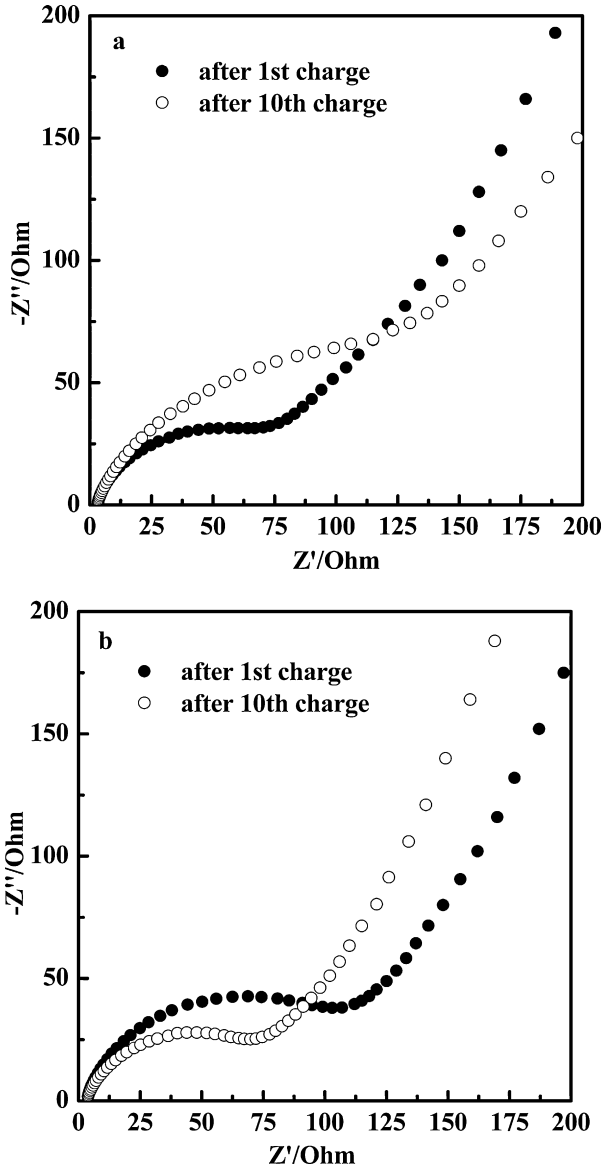

Fig. 6. Nyquist plots for PMLSF electrodes charged to 1.4 V after the first and tenth cycle in VC-free electrolyte (a) and in VC-containing electrolyte (b).

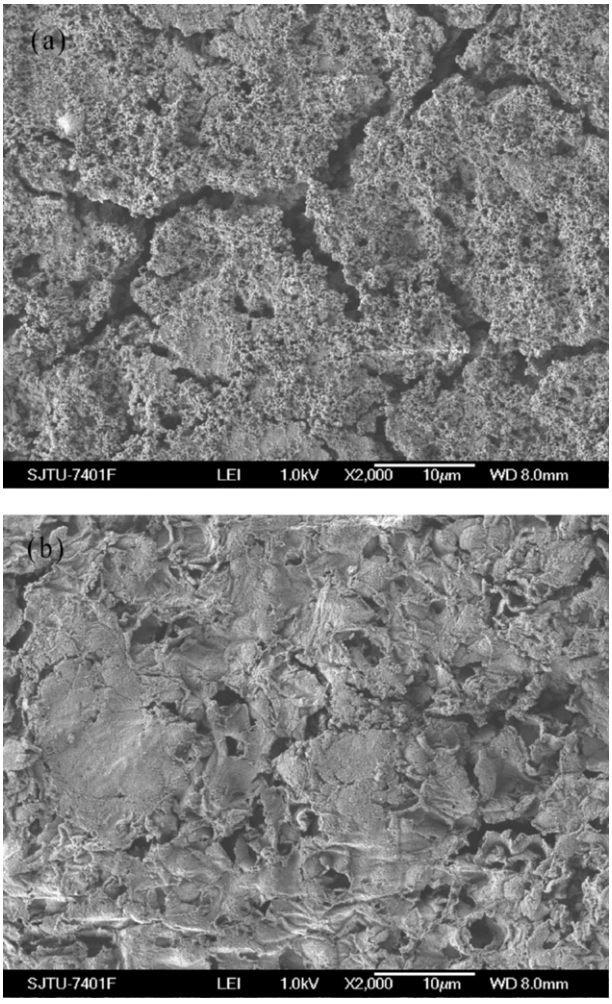

Fig. 7. SEM images of PMLSF electrodes after 50 cycles in VC-free electrolyte (a) and VC-containing electrolyte (b).

by gradual activation of the electrode on the premise of the more stable electrode structure and SEI protection film.

The positive effect of VC additive can be further illustrated by the morphology of the PMLSF electrodes after cycling. Fig. 7 gives the SEM images of the PMLSF electrodes after 50 cycles in VC-free and VC-containing electrolytes. Because of the volume change during lithium insertion/extraction and the formation of SEI layer, the original microspheres feature disappears from the surface for both the PMLSF electrodes. Using VC-free electrolyte, the Li–Si film presents a rough and porous morphology with the serious cracks in a width of ca. 1 μm and length of ca. 10 μm, which reveals the deterioration of the electrode structure and lack of entire SEI layer. By contrast, the surface morphology of the PMLSF electrode is smoother and the cracks are not apparent in VC-containing electrolyte. VC-derived multi-components SEI layer has been analyzed by a series of methods and the related reaction mechanism discussed [23]. The authors also revealed that effective SEI formation by the reduction of VC took place at more than 1 V vs. Li/Li^+ and before that of EC, so that the reductive gases of the EC and DMC solvents such as C_2H_4, CH_4, and CO can be suppressed. We believe that less gas release and VC-derived polymers and organic lithium salts may result in a more compact and stable SEI layer, which can not only reinforce the structure stability of the PMLSF electrode, but also suppress a continuous decomposition of the electrolyte during cycling. These may be the reason for the positive effect of VC additive. In fact, the average charge–discharge efficiency except for the first cycle is 96.1% in VC-free electrolyte, but it reaches 97.8% in VC-containing electrolyte. For the long-term cycling stability, a dense but also flexible SEI layer is necessary to follow volume change of the Si-based electrode during cycling, keep its integrity and prevent any electrolyte decomposition.

4. Conclusions

The porous-microspheres Li–Si films (PMLSF) as negative electrodes of lithium-ion batteries can be electrodeposited on Cu foil substrate by a multi-step constant current technique. The particular film morphology (i.e., porous particle structure with inter-particle free space) can buffer the volume change during the lithium insertion/extraction process and favor a stable cycling behavior. The co-deposition of Li and Si greatly suppresses the initial irreversiblity capacity caused by defects and reactive impurities in the PMLSF and simultaneously induces a formation of SEI layer on the electrode. As a result, a high coulombic efficiency more than 90% is obtainable at the first cycle. Moreover, when the PMLSF electrode is cycled in VC-containing electrolyte, an excellent cycling performance can

be achieved. After 50 cycles, 96.0% of the initial charge capacity remains. The positive effect of VC additive may be attributed to the reinforced SEI layer via its decomposition product.

Acknowledgement

This work was financially supported by NSFC (20873085).

References

[1] M.D. Fleischauer, J. Li, M.J. Brett, J. Electrochem. Soc. 156 (2009) A33–36.
[2] S.K. Cheah, E. Perre, M. Rooth, M. Fondell, A. Harsta, L. Nyholm, M. Boman, T. Gustafsson, J. Lu, P. Simon, K. Edstrom, Nano Lett. 9 (2009) 3230–3233.
[3] M. Winter, J.O. Besenhard, M.E. Spahr, P. Novak, Adv. Mater. 10 (1998) 725–763.
[4] H. Kim, B. Han, J. Choo, J. Cho, Angew. Chem. Int. Ed. 47 (2008) 10151–10154.
[5] A. Magasinski, P. Dixon, B. Hertzberg, A. Kvit, J. Ayala, G. Yushin, Nat. Mater. 9 (2010) 353–358.
[6] Y.S. Hu, R. Dezan-Cakan, M.M. Titirici, J.O. Muller, R. Schlogl, M. Antonietti, J. Maier, Angew. Chem. Int. Ed. 47 (2008) 1645–1649.
[7] L.B. Chen, K. Wang, X.H. Xie, J.Y. Xie, J. Power Sources 174 (2007) 538–543.
[8] T. Takamura, S. Ohara, M. Uehara, K. Sekine, J. Power Sources 129 (2004) 96–100.
[9] H.J. Ahn, Y.S. Kim, K.W. Park, T.Y. Seong, Chem. Commun. (2005) 43–45.
[10] J.T. Yin, M. Wada, K. Yamamoto, Y. Kitano, S. Tanase, T. Sakai, J. Electrochem. Soc. 153 (2006) A472–A477.
[11] M.D. Fleischauer, M.N. Obrovac, J.R. Dahn, J. Electrochem. Soc. 155 (2008) A851–A854.
[12] S.W. Song, K.A. Striebel, R.P. Reade, G.A. Roberts, E.J. Cairns, J. Electrochem. Soc. 150 (2003) A121–A127.
[13] Q.M. Pan, H.B. Wang, Y.H. Jiang, Electrochem. Commun. 9 (2007) 754–760.
[14] I.W. Seong, K.T. Kim, W.Y. Yoon, J. Power Sources 189 (2009) 511–514.
[15] I.W. Seong, W.Y. Yoon, J. Power Sources 195 (2010) 6143–6147.
[16] J. Yang, Y. Takeda, N. Imanishi, O. Yamamoto, J. Electrochem. Soc. 147 (2000) 1671–1676.
[17] D. Aurbach, M.L. Daroux, P.W. Faguy, E. Yeager, J. Electrochem. Soc. 134 (1987) 1611–1620.
[18] H.-C. Shin, J. Dong, M.L. Liu, Adv. Mater. 15 (2003) 1610–1614.
[19] Y. Nishimura, Y. Fukunaka, Electrochim. Acta 53 (2007) 111–116.
[20] T. Munisamy, A.J. Bard, Electrochim. Acta 55 (2010) 3797–3803.
[21] J.P. Maranchi, A.F. Hepp, P.N. Kumta, Electrochem. Solid-State Lett. 6 (2003) A198–A201.
[22] P.F. Gao, J.W. Fu, J. Yang, R.G. Lv, J.L. Wang, Y.N. Nuli, X.Z. Tang, Phys. Chem. Chem. Phys. 11 (2009) 11101–11105.
[23] H. Ota, Y. Sakata, A. Inoue, S. Yamaguchi, J. Electrochem. Soc. 151 (2004) A1659–A1669.